Disruption of gray matter microstructure in Alzheimer's disease continuum using fiber orientation

Peter Lee
Korea Advanced Institute of Science and Technology https://orcid.org/0000-0001-5433-1882
Hang-Rai Kim
Korea Advanced Institute of Science and Technology
Yong Jeong (yong@kaist.ac.kr)
https://orcid.org/0000-0002-5907-3787

Research article

Keywords: Alzheimer's disease, Early diagnosis, Diffusion tensor imaging, Microstructure, Biomarkers

Posted Date: March 16th, 2020

DOI: https://doi.org/10.21203/rs.3.rs-17303/v1

Version of Record: A version of this preprint was published on October 2nd, 2020. See the published version at https://doi.org/10.1186/s12883-020-01939-2.

Abstract

There have been several MR imaging biomarkers of Alzheimer's disease (AD) for early diagnosis. Cortical mean diffusivity (MD) is one of them for the study of the cortical microstructural change in AD. However, several factors may overshadow the feasibility of MD as AD biomarker. Thus, current study investigated feasible gray matter microstructure biomarker with higher sensitivity for early AD detection. With the aim of facilitating the early detection of AD, the Alzheimer's Disease Neuroimaging Initiative (ADNI) proposed two stages based on the memory performance: early mild cognitive impairment (EMCI) and late mild cognitive impairment (LMCI). We propose single shell DTI measure, ' radiality ', for early AD biomarker. It is a dot product between cortical surface normal vector and primary diffusion direction, which presumably reflects the fiber orientation within the cortical column. Here, we gathered images from ADNI phase 2 & 3; 78 cognitive normal, 51 EMCI, 34 LMCI, and 39 AD patients. Then, we evaluated cortical thickness (CTh), MD, amount of amyloid and tau accumulations using PET, which are conventional AD biomarkers. Radiality was projected on gray matter surface to compare and validate the changes along other neuroimage biomarkers. Results showed decreased radiality primarily in entorhinal, insula, frontal and temporal cortex as disease progress onward. Especially, radiality could delineate the difference between cognitive normal and EMCI group while other biomarkers could not. We looked into the relationship between the radiality and other biomarkers to validate its pathological evidence in AD. Overall, radiality showed high association with conventional biomarkers. Additional ROI analysis exhibit dynamics of AD related changes as stages onward. In conclusion, radiality in cortical gray matter showed AD specific changes and relevance with other conventional AD biomarkers with higher sensitivity. Besides, it could show group differences in early AD changes from EMCI which show advantage for early diagnosis than using conventional biomarkers. We provide the evidence of structure changes with cognitive impairment and suggest radiality as a sensitive biomarker for early diagnose and progress monitor AD.

1. Background

Alzheimer's disease (AD) has a long preclinical period where several pathophysiological changes occur before the main symptom. As progress of AD is not completely understood, it makes early diagnosis and intervention difficult [1, 2]. Repetitive failures of recent drug trials attribute to applying treatment to patients at the progressed stage [3–5]. Thus, identification of people at the earlier stage is critical in clinical trials and may be promising for controlling this devastating disease.

At present, there are several biomarkers to diagnose and monitor disease progression; amyloid and tau deposit through PET imaging or from cerebrospinal fluid (CSF), volumetric and morphology analysis using T1 weighted MR imaging and clinical assessments. The Alzheimer's disease Neuroimaging Initiative (ADNI) proposed two stages–early mild cognitive impairment (EMCI) and late mild cognitive impairment (LMCI)–based on the memory performance [6–7]. Patients with EMCI and LMCI were subdivided solely on the score of the memory scale, but other biomarkers such as the hippocampal volume and CSF biomarkers also showed continuous trajectories suggesting that EMCI could be an

earliest stage of AD [8]. Thus, evaluating the differences between EMCI and LMCI might help understanding the early stage disease progression.

Diffusion tensor image (DTI) is sensitized to the motion of water molecules as they interact within tissues, thus reflecting characteristics of their immediate structural surroundings [9, 10], thus widely used for studying white matter integrity. Early studies using DTI in AD have focused mostly on white matter using fractional anisotropy. However, since white-matter changes in AD may be the results of Wallerian degeneration, followed by the loss of cortical neurons in gray matter [11, 12], the destruction of white matter is a less sensitive change in AD.

The idea of measuring microstructural changes in grey matter using DTI has been demonstrated in both AD and frontotemporal dementia [13–15]. These studies showed that gray matter mean diffusivity (MD) is increased in patients compared with healthy control and MD could be a promising imaging biomarker. However, some studies suggested that increased MD could be a spilled over effect from CSF and this effect persisted even with rigorous correction such as partial volume effect correction [16].

To overcome this problem, we used radiality, which is presumably reflecting the integrity of tangential cortical fibers. This parameter has been applied to study neurodevelopment and could distinguish stages of aging [17–19]. Moreover, cortical microstructural changes are often observed with aging or neurodegeneration, which can be opposite of neurodevelopment [20–22]. Thus, changes of fiber orientation may suggest cortical disruption and feasibility of radiality as a biomarker in the neurodegenerative disorders.

In this study, we hypothesized that the radiality of the gray matter could be a microstructure measure of cortex and used as the early signature of AD. We performed a cross-sectional surface-based cortical analysis approach using DTI, amyloid PET, and Tau PET images to a population of patients with AD continuum. We evaluated whether gray matter radiality shows: i) early mesoscopic changes in regions known to undergo early AD-related pathological change, and ii) compliment to conventional AD biomarkers while providing a distinct information regarding AD-related pathologies.

2. Methods

2.1 Demographics

Data used in preparation of this article were obtained from Alzheimer's Disease Neuroimaging Initiative (ADNI) database (adni.loni.usc.edu). Among ADNI phase 2 & 3 database, we analyzed the subjects who took both MRI and PET (amyloid, AV 45 and tau, AV 1451); 78 cognitive normal (CN), 51 EMCI, 34 LMCI, and 39 AD. Subjects were sampled with following criteria; age around 60 to 90 year old, education year 12 to 20, and gender match within group. To assess AD continuum, amyloid negative CN and amyloid positive EMCI, LMCI, and AD subjects were selected. A total of 202 subjects' T1 and DTI images were gathered from ADNI. To increase sample size, multi-center approach was used. Following clinical and neuropsychological assessments were included: global clinical dementia ratings (GCDR), Mini Mental

State Examination (MMSE), Modified Alzheimer Disease Assessment Scale cognitive subscale (MADAS-Cog), and Wechsler Memory Scale Logical Memory I & II. AV45 amyloid PET image data were acquired from the ADNI database with positivity cutoff of 1.11. Demographics of included subjects are presented in Table 1. Note that subjects who underwent AV1451 tau PET imaging were 44 in CN, 9 in EMCI, 5 in LMCI, and 3 in AD. Additional 28 CN subjects who showed amyloid positive were gathered to see earliest AD pathological changes as presented in Supp. Table 1.

Table 1

Demographics

	CN (n = 78)	EMCI (n = 50)	LMCI (n = 34)	AD (n = 39)	Post hoc
Female, n (%)	42 (53.8)	19 (37.2)	15 (44.1)	17 (43.6)	–
Age (SD) (y)	72.7 ± 5.9	74.7 ± 5.3	73.9 ± 5.6	74.7 ± 7.17	–
Education (SD) (y)	16.67 ± 2.5	15.2 ± 2.6	16.1 ± 2.7	15.4 ± 2.9	–
GCDR (SD)	0.0	0.5	0.5	0.8 ± 0.3	CN < EMCI = LMCI < AD
MMSE (SD)	28.6 ± 1.1	28.4 ± 1.4	22.3 ± 1.9	20.1 ± 1.9	CN = EMCI = LMCI < AD
MADAS-Cog (SD)	6.4 ± 3.1	10.3 ± 6.7	19.5 ± 6.1	28.5 ± 9.8	CN < EMCI < LMCI < AD
Logical memory I: Immediate recall (SD)	13.3 ± 3.0	10.5 ± 2.3	5.8 ± 3.1	3.5 ± 2.0	CN < EMCI < LMCI < AD
Logical memory II: Delayed recall (SD)	11.8 ± 3.3	9.2 ± 1.4	2.5 ± 2.9	1.6 ± 2.0	CN < EMCI < LMCI = AD
MRI center	30/48	41/10	28/6	36/3	
Florbetapir+	0 (0)	50 (100)	34 (100)	39 (100)	–
Subjects with AV1451 image	44 (68.8)	9 (14.1)	5 (7.8)	3 (4.7)	–
	N	**Accuracy**	**Sensitivity**	**Specificity**	**AUC**
CN vs EMCI	78 vs 51	70.5%	70.2%	72.7%	0.766
CN vs LMCI	78 vs 34	67.9%	70.6%	66.7%	0.757
CN vs (EMCI + LMCI)	78 vs 85	70.5%	69.4%	66.7%	0.766

Data are n (%) or mean ± SD values. There were no gender, age, or education intergroup differences. MMSE scores in CN, EMCI, and LMCI did not show significant differences. Logical Memory II: delayed recall in LMCI and AD did not show a significant difference. For MRI data, two major scanner were used: GE and SIMENS and delineated as MRI center GE/SIMENS.

AD: Alzheimer's disease, CN: cognitive normal, EMCI: early mild cognitive impairment, GCDR: global Clinical Dementia Rating, LMCI: late mild cognitive impairment, MADAS-Cog: Modified Alzheimer's Disease Assessment Scale-Cognitive subscale, MMSE: Mini Mental State Examination.

	CN (n = 78)	EMCI (n = 50)	LMCI (n = 34)	AD (n = 39)	Post hoc
CN vs AD	78 vs 39	78.6%	79.5%	78.1%	0.867
CN vs (EMCI + LMCI + AD)	78 vs 124	72.8%	72.3%	73.1%	0.798
Data are n (%) or mean ± SD values. There were no gender, age, or education intergroup differences. MMSE scores in CN, EMCI, and LMCI did not show significant differences. Logical Memory II: delayed recall in LMCI and AD did not show a significant difference. For MRI data, two major scanner were used: GE and SIMENS and delineated as MRI center GE/SIMENS.					
AD: Alzheimer's disease, CN: cognitive normal, EMCI: early mild cognitive impairment, GCDR: global Clinical Dementia Rating, LMCI: late mild cognitive impairment, MADAS-Cog: Modified Alzheimer's Disease Assessment Scale-Cognitive subscale, MMSE: Mini Mental State Examination.					

2.2 Image processing

T1 weighted images were processed with Freesurfer package v6.0 (http://surfer.nmr.mgh.harvard.edu) using procedure as previously reported [13]. Cortical thickness (CTh) maps were registered to Freesurfer average sphere through spherical registration for group comparison. DTI and PET images were registered with their respect to T1 images using boundary-based algorithm for further process. DTI images were processed using FSL package as followed: eddy current correction, rotate gradient vectors from the results of eddy correction, and tensor fitting to produce mean diffusivity map and primary eigenvector map. DTI metrics were further processed to avoid partial volume effect using Koo et al [24]. PET images were partial volume corrected using mri_gtmpvc which is built in Freesurfer package. PET images were normalized by mean signal from whole cerebellum and used as standardized uptake value ratio (SUVR) for amyloid and tau PET, AV45 and AV1451 respectively. Then images were boundary-based registered to respective T1 structural image. To avoid any partial volume effects, the deepest parts of the gray matter were analyzed. Figure 1 shows the overall scheme of the process. Lastly, CTh was smoothed with 10 mm while other modalities were smoothed with 15 mm full width half maximum Gaussian kernel.

2.3 Calculation of radiality

A surface normal vector was obtained from individual gray matter surface to define cortical orientation. Vertex-wise dot product between primary eigenvector of diffusion tensor and the surface normal vector was quantified as a radiality index; r: where v represents surface normal vector and e1 represents primary diffusion direction [20].

$$r = |\widehat{v_n} \cdot \widehat{e_1}|$$

It ranges from 0 to 1, where r = 0 indicates tangential diffusion and r = 1 indicates radial diffusion to cortex. Subject's principal eigenvector map was projected onto the individual surface reconstruction to

calculate vertex-wise radiality as discussed in [20].

2.4 Statistical analysis

We first compared the differences between groups for radiality, CTh, MD, AV45 and AV1451 with a two-class general linear model, as implemented in Freesurfer. The results were cluster-wise corrected for family-wise error corrected p-value < 0.05

To assess the relationship between radiality and other neuroimage biomarkers, a vertex by vertex partial correlation was computed between the radiality, CTh, MD, AV45, and AV1451 values. Specifically, a general linear model was created, being radiality the dependent variable of interest, using other biomarkers as the independent variable, and introducing age, gender, and year of education as nuisance variables.

All the group analyses included age, gender, year of education, and MRI center as covariates. To avoid false positives, a Monte Carlo simulation with 10,000 repeats as implemented in Freesurfer (family-wise error [FWE], P < .05) was tested. Only those regions that survived those multiple comparisons are shown in the figures.

To assess the linear relationship between radiality and other neuroimage biomarkers, mean metrics within AD specific ROIs were quantified. ROIs include entorhinal, fusiform, insula, inferior, middle, and superior temporal cortex. Mean metrics within ROI were plotted in a box and whisker plots. Significance between groups was tested with one-way ANOVA.

3. Results

3.1 Group comparison along AD continuum

We first compared radiality, CTh, and MD differences between groups; CN vs EMCI, CN vs LMCI, CN vs AD as respectively. The results were cluster-wise corrected for family-wise error corrected p-value < 0.05. Figure 2 shows significant group different clusters range from p-value 0.05 to 10^{-5}. Only radiality could delineate the difference from EMCI to CN. Compared to CN, all groups showed decreased radiality, decreased CTh, and increased MD. There were no group difference of radiality in EMCI and LMCI.

3.2 Partial correlation between radiality and other image biomarkers

We then found vertex-wise correlation between image biomarkers and radiality. CTh showed mostly positive correlations that decrease in cortical thickness accompanied with decrease in radiality. MD showed mostly negative correlation that increase in MD accompanied with decrease in radiality. Amyloid and tau levels showed negative correlation with radiality (Fig. 3).

3.3 Correlations between image biomarkers and radiality

In order to find progressive changes in radiality as disease progression, AD specific ROIs mask was used to calculate mean biomarker data. Each subject's mean data were scatter plotted and used to calculate Pearson correlation. CTh showed R = 0.641, MD showed R = -0.677, AV45 showed R = -0.490, and AV1451 showed R = -0.412 with radiality (Fig. 4).

3.4 Radiality dynamics from AD specific ROIs

To find generative changes in radiality as disease progresses, mean radiality in AD ROIs was calculated for direct comparison among groups. Radiality within AD specific ROIs were plotted in a box and whisker plot. It shows that the radilaity is decreasing linearly with disease progression.

When see the change of radilatiy in each ROI, most of the ROIs showed characteristic of disease progression as decrease in radiality. Significance was tested with one-way ANOVA with $P < 0.05$, 0.01, 0.001. Insula, middle and superior temporal cortex showed most radiality reduction with disease onward.

3.5 Cut-off analysis using Radiality

To further test feasibility of radiality as AD biomarker, we performed cut-off analysis to distinguish CN with other AD stages (Supp. Table 2.). We sought to find the cur-off that minimize the difference between sensitivity and specificity, cost effective point. With varying cut-off, we could quantify ROC curve and calculated AUC. Classification of CN vs EMCI showed 70.5% accuracy with 70.2% sensitivity, 72.7% specificity, and 0.766 AUC. Given that sample size was relatively small (CN N = 78, EMCI N = 51), result showed promising aspect of radiality as biomarker. Subsequent analysis to distinguish LMCI, EMCI + LMCI, AD, and EMCI + LMCI + AD also showed similar results.

4. Discussion

In this study, we tried to identify the early features of EMCI using cortical radiality, which reflects mesoscopic structural changes. By leveraging the radiality in the gray matter, we could detect the changes in EMCI which were not detected by conventional MRI biomarkers. To the best of our knowledge, this is the first study, which applied gray matter radiality in neurodegenerative disease and detected significant mesoscopic changes in EMCI using MRI. In our study, we found progressively larger regions of decreased radiality as disease progresses, starting from medial temporal cortex in EMCI to whole brain in AD. While, CTh or MD of EMCI did not show significant difference with CN.

We investigated the relationship of radiality with other image measures. Association between radiality and CTh showed strong positive correlation on widespread regions of the brain as shown in Fig. 3. It is clear that higher CTh indicate deeper cortical structure and fiber orientation tend to have radial orientation. Cortical depth profile analysis showed that thicker the cortical thickness larger the radiality [25]. In addition, MD showed strong negative correlation on mostly temporal, parietal, and frontal cortices.

Radiality may sensitive to CTh but reflecting microstructural feature as well. With AV45 and AV1451, radiality showed association that widely overlapped with both CTh and MD. It should be noted that there were few tau PET images were available. Radiality may also reflect changes due to accumulation of pathologic protein accumulation within the cortex.

Although microstructural changes associated with radiality is unclear, one plausible feature is the disorganization of tangential cortical fibers. It has been reported that the presence of tangential cortical fibers distinguishes stages of neurodevelopment and aging. There are several events that lead to increase in tangentially oriented fibers including dendritic elaboration [26], formation of local circuits [27], addition of thalamo-cortical fibers [28] and disappearance of radial glia [29, 30]. Decrease in radiality may indicate reversal of the events that take place during neurodevelopment. For instance, synaptic loss, neuronal soma changes and neurite disorganization occurs along with the neuronal loss may lead to decrease in radiality. These changes may concurrent with net loss of macromolecule that affect diffusivity, increasing free water in extracellular space. However, radiality provide evidence of neuronal density that explain concurrent cortical atrophy. Furthermore, accumulation of amyloid or tau proteins may also participate in the disruption of microstructure. Given radiality can delineate the EMCI, we can further speculate that these microstructural changes occur in the earlier stage of AD which are not apparent in macroscopic investigation.

To test the sensitivity of radiality, we sought to find earliest stage of AD. Interestingly, our CN vs EMCI cluster analysis did not show biphasic trajectory as discussed in previous work [31]. Thus, we conducted additional analysis on amyloid negative CN and amyloid positive CN (Supp Fig. 1). We could observe biphasic behavior of CTh and MD where biomarkers showed opposite direction of changes. While CTh showed increased and MD decreased, radiality showed monotonous decrease in amyloid positive CN. This distinct behavior of radiality could characterize the changes in EMCI while CTh and MD could not. Both the CTh increase and MD decrease in early stage of AD was thought to be caused by an amyloid-induced inflammatory response. However, radiality seems to decrease whenever there is microstructural changes in the tissue. From preterm study, occipital cortex showed decrease in radiality as in early development [17–19]. At early stage, the extracellular water is hindered orthogonal to the fibers, and thus has a principal direction of diffusivity that augments the radial structure of the intra-cellular compartment.

In short, radiality could discriminate EMCI from CN and exhibited property of reflecting early disease progression. Previous study showed inverse change of CTh and MD in early stage of AD [31]. Such regions of change in radiality were entorhinal cortex, parahippocampal gyrus, middle temporal gyrus, superior and middle frontal gyrus and the supramarginal gyrus bilaterally; a pattern which is similar to that seen in studies of cortical thickness [32]. That is, we could confirm that EMCI may predate LMCI in the perspective of disease progression.

There were several limitations of the current study. First, use of multi-protocol DTI images could influence the observation of progressive changes in MCI. We sought to control age, gender, year of education, and

center variate among the group while applying ComBat to minimize the variation between subjects [33]. Second, number of subjects who took AV1451 imaging were not enough to show the relationship with tau pathology. In order to focus on progressive changes, not only showing relationship with AV45 but also with AV1451 is important aspect [34]. However, several subjects in this study underwent screening only once without follow up or only MRI data were available.

5. Conclusions

In conclusion, we investigated the cortical changes in EMCI using structural MRI and DTI as well as PET imaging markers. Only radiality could delineate the changes in EMCI while cortical thickness and MD could not. In addition, radiality changes in frontal cortex as simultaneously with AV45 in continuum. These results indicate that multimodal approach, atrophy and microstructure, may illuminate early changes in AD. However, further study is needed to support this diffusion orientation change. We also demonstrate that the orientation changes in AD specific ROIs to overcome cluster analysis, indicating possible use of it as a biomarker for AD progression.

Abbreviations

AD Alzheimer's disease

MD Mean diffusivity

ADNI Alzheimer's Disease Neuroimaging Initiative

EMCI Early mild cognitive impairment

LMCI Late mild cognitive impairment

CTh Cortical thickness

CSF Cerebrospinal fluid

DTI Diffusion tensor imaging

CN Cognitive normal

GCDR Global clinical dementia ratings

MMSE Mini Mental State Examination

MADAS-Cog Modified Alzheimer's disease Assessment Scale cognitive subscale

SUVR Standardized uptake value ratio

Declarations

Ethical approval and consent to participate

The study procedures were approved by the institutional review boards of all participating centers (https://adni.loni.usc.edu/wp-content/uploads/how_to_apply/ ADNI_Acknowledgement_List.pdf), and written informed consent was obtained from all participants or their authorized representatives. Ethics approval was obtained from the institutional review boards of each institution involved: Oregon Health and Science University; University of Southern California; University of California—San Diego; University of Michigan; Mayo Clinic, Rochester; Baylor College of Medicine; Columbia University Medical Center; Washington University, St. Louis; University of Alabama at Birmingham; Mount Sinai School of Medicine; Rush University Medical Center; Wien Center; Johns Hopkins University; New York University; Duke University Medical Center; University of Pennsylvania; University of Kentucky; University of Pittsburgh; University of Rochester Medical Center; University of California, Irvine; University of Texas Southwestern Medical School; Emory University; University of Kansas, Medical Center; University of California, Los Angeles; Mayo Clinic, Jacksonville; Indiana University; Yale University School of Medicine; McGill University, Montreal-Jewish General Hospital; Sunnybrook Health Sciences, Ontario; U.B.C.Clinic for AD & Related Disorders; Cognitive Neurology—St. Joseph's, Ontario; Cleveland Clinic Lou Ruvo Center for Brain Health; Northwestern University; Premiere Research Inst (Palm Beach Neurology); Georgetown University Medical Center; Brigham and Women's Hospital; Stanford University; Banner Sun Health Research Institute; Boston University; Howard University; Case Western Reserve University; University of California, Davis—Sacramento; Neurological Care of CNY; Parkwood Hospital; University of Wisconsin; University of California, Irvine—BIC; Banner Alzheimer's Institute; Dent Neurologic Institute; Ohio State University; Albany Medical College; Hartford Hospital, Olin Neuropsychiatry Research Center; Dartmouth-Hitchcock Medical Center; Wake Forest University Health Sciences; Rhode Island Hospital; Butler Hospital; UC San Francisco; Medical University South Carolina; St. Joseph's Health Care Nathan Kline Institute; University of Iowa College of Medicine; Cornell University; and University of South Florida: USF Health Byrd Alzheimer's Institute. Upon accessing the database, we have received administrative approval for access to the ADNI database.

Consent for publication

Not applicable

Availability of data and materials

The MRI and PET data were downloaded from the Alzheimer's Disease Neuroimaging Initiative (ADNI) database (http://adni.loni.usc.edu/). Application for access to the ADNI data can be submitted by anyone at http://adni.loni.usc.edu/data-samples/access-data/. The process includes completion of an online application form and acceptance of Data Use Agreement. We have received administrative approval for access to the ADNI database.

Competing interests

The authors declare that they have no competing interests.

Funding

Data analysis, result interpretation, and manuscript writing were supported in part by grant HI14C2768 from the Korea Health Technology Research and Development Project through the Korea Health Industry Development Institute, funded by the Ministry of Health & Welfare, Republic of Korea. Data analysis, method development, and manuscript writing were supported in part by the Bio & Medical Technology Development Program (2016941946) through the National Research Foundation of Korea (NRF), funded by the Ministry of Science, ICT and Future Planning.

Data collection and designing for this project was funded by the Alzheimer's Disease Neuroimaging Initiative (ADNI) (National Institutes of Health Grant U01 AG024904) and DOD ADNI (Department of Defense award number W81XWH-12-2-0012). ADNI is funded by the National Institute on Aging, the National Institute of Biomedical Imaging and Bioengineering, and through generous contributions from the following: AbbVie, Alzheimer's Association; Alzheimer's Drug Discovery Foundation; Araclon Biotech; BioClinica, Inc.; Biogen; Bristol-Myers Squibb Company; CereSpir, Inc.; Eisai Inc.; Elan Pharmaceuticals, Inc.; Eli Lilly and Company; EuroImmun; F. Hoffmann-La Roche Ltd and its affiliated company Genentech, Inc.; Fujirebio; GE Healthcare; IXICO Ltd.; Janssen Alzheimer Immunotherapy Research & Development, LLC.; Johnson & Johnson Pharmaceutical Research & Development LLC.; Lumosity; Lundbeck; Merck & Co., Inc.; Meso Scale Diagnostics, LLC.; NeuroRx Research; Neurotrack Technologies; Novartis Pharmaceuticals Corporation; Pfizer Inc.; Piramal Imaging; Servier; Takeda Pharmaceutical Company; and Transition Therapeutics. The Canadian Institutes of Health Research is providing funds to support ADNI clinical sites in Canada. Private sector contributions are facilitated by the Foundation for the National Institutes of Health (www.fnih.org). The grantee organization is the Northern California Institute for Research and Education, and the study is coordinated by the Alzheimer's Disease Cooperative Study at the University of California, San Diego. ADNI data are disseminated by the Laboratory for Neuro Imaging at the University of Southern California.

Authors' contributions

PL, YJ, and HK contributed to the study conception and design. Material preparation, data collection and analysis were performed by PL. The first draft of the manuscript was written by PL and YJ and HK commented on previous versions of the manuscript. All authors read and approved the final manuscript.

Acknowledgement

Data used in preparation of this article were obtained from the Alzheimer's Disease Neuroimaging Initiative (ADNI) database (adni.loni.usc.edu). As such, the investigators within the ADNI contributed to the design and implementation of ADNI and/or provided data but did not participate in analysis or writing

of this report. A complete listing of ADNI investigators can be found at: http://adni.loni.usc.edu/wp-content/uploads/how_to_apply/ADNI_Acknowledgement_List.pdf

References

1. Jack CR Jr, Knopman DS, Jagust WJ, Shaw LM, Aisen PS, Weiner MW, et al. Hypothetical model of dynamic biomarkers of the Alzheimer's pathological cascade. Lancet Neurol 9 (2010), pp. 119-128.
2. Shim YS, Morris JC. Biomarkers predicting Alzheimer's disease in cognitively normal aging. J Clin Neurol 7 (2011), pp. 60-68.
3. Cummings JL, Morstorf T, Zhong K, Alzheimer's disease drug-development pipeline: few candidates, frequent failures, Alzheimer's Research & Therapy, 6 (2014) 37 doi:10.1186/alzrt269
4. Anderson RM, Hadjichrysanthou C, Evans, S, Wong, MM, Why do so many clinical trials of therapies for Alzheimer's disease fail? Lancet, 390 (2017) pp. 2327-2329 doi:10.1016/S0140-6736(17)32399-1
5. Schott JM, Aisen PS, Cummings JL, Howard RJ, Fox NC. Unsuccessful trials of therapies for Alzheimer's disease. Lancet 2019 393:29 doi:10.1016/S0140-6736(18)31896-8
6. Aisen PS, Petersen RC, Donohue MC, Gamst A, Raman R, Thomas RG, et al. Clinical core of the Alzheimer's Disease neuroimaging initiative: progress and plans. Alzheimer's Dementia *6 (*2010), pp. 239-246.
7. Weiner MW, Aisen PS, Jack CR Jr, Jagust WJ, Trojanowski JQ, Shaw L, et al. The Alzheimer's disease neuroimaging initiative: progress report and future plans. Alzheimer's Dementia*,* 6 (2010) pp. 202-211
8. Qiu Y, Li L, Zhou TY, Lu W, Alzheimer's Disease Neuroimaging Initiative. Alzheimer's disease progression model based on integrated biomarkers and clinical measures. Acta Pharmacol Sin 35 *(*2014), pp. 1111- 1120.
9. Basser PJ, Mattiello J, LeBihan D, MR diffusion tensor spectroscopy and imaging, Biophys. J. 66 (1994) 259–267.
10. Pierpaoli C, Basser PJ, Toward a quantitative assessment of diffusion anisotropy, Magn. Reson. Med. 36 (1996) 893–906.
11. Bozzali M, Cercignani M, Sormani MP, Comi G, Filippi M. Quantification of brain gray matter damage in different ms phenotypes by use of diffusion tensor MR imaging. Am. J. Neuroradiol. 2002;23:985–988
12. ColemanMP, FreemanMR. Wallerian degeneration, wld(s), and nmnat. Annu Rev Neurosci2010;33:245-267.
13. Montal V, Vilaplana E, Alcolea D, Pegueroles J, Pasternak O, González-Ortiz S, et al., Cortical microstructural changes along the Alzheimer's disease continuum, Alzheimers Dement., 14 (2018), pp. 340-351
14. Illán-Gala I, Montal V, Borrego-Écija S, et al. Cortical microstructure in the behavioural variant of frontotemporal dementia: looking beyond atrophy. Brain 2019; 142: 1121– 1133.

15. Lee P, Ryoo H, Park J, Jeong Y, Alzheimer's Disease Neuroimaging Initiative. Morphological and Microstructural Changes of the Hippocampus in Early MCI: A Study Utilizing the Alzheimer's Disease Neuroimaging Initiative Database. J Clin Neurol. 2017 Apr;13(2):144-154.
16. Henf J, Grothe MJ, Brueggen K, Teipel S, Dyrba M. Mean diffusivity in cortical gray matter in Alzheimer's disease: the importance of partial volume correction. Neuroimage Clin. 2018;17:579–86.
17. Eaton-Rosen Z, Scherrer B, Melbourne A, Ourselin S, Neil JJ, Warfield SK, Investigating the maturation of microstructure and radial orientation in the preterm human cortex with diffusion MRI, Neuroimage, 162 (2017), pp. 65-72
18. Kroenke CD, Using diffusion anisotropy to study cerebral cortical gray matter development, J. Mag. Res. 292 (2018), pp. 106-116
19. Dean DC III, O'Muircheartaigh J, Dirks H, et al. Mapping an index of the myelin g-ratio in infants using magnetic resonance imaging. Neuroimage. 2016; 132: 225- 237
20. McNab, Jennifer A et al. Surface based analysis of diffusion orientation for identifying architectonic domains in the in vivo human cortex. NeuroImage vol. 69 (2013): 87-100. doi:10.1016/j.neuroimage.2012.11.065
21. Fukutomi H, Glasser MF, Zhang H, Autio JA, Coalson TS, Okada T, et al. Neurite imaging reveals microstructural variations in human cerebral cortical gray matter Neuroimage, 182 (2018), pp. 488-499
22. Wu D et al. Localized diffusion magnetic resonance micro-imaging of the live mouse brain. NeuroImage vol. 91 (2014): 12-20. doi:10.1016/j.neuroimage.2014.01.014
23. Szczepankiewicz F et al. Quantification of microscopic diffusion anisotropy disentangles effects of orientation dispersion from microstructure: applications in healthy volunteers and in brain tumors. NeuroImage vol. 104 (2015): 241-52. doi:10.1016/j.neuroimage.2014.09.057
24. Koo BB, Hua N, Choi CH, Ronen I, Lee JM, Kim DS (2009) A framework to analyze partial volume effect on gray matter mean diffusivity measurements. Neuroimage 44:136–144, doi:10.1016/j.neuroimage.2008.07.064
25. Truong TK, Guidon A, and Song AW. (2014). Cortical depth dependence of the diffusion anisotropy in the human cortical gray matter in vivo. PLoS ONE 9:e91424. doi: 10.1371/journal.pone.0091424
26. Marín-Padilla M, Ontogenesis of the pyramidal cell of the mammalian neocortex and developmental cytoarchitectonics: a unifying theory. J Comp Neurol. 1992 Jul 8; 321(2):223-40.
27. Callaway EM, Katz LC, Emergence and refinement of clustered horizontal connections in cat striate cortex. J Neurosci. 1990 Apr; 10(4):1134-53.
28. Ghosh A, Shatz CJ. A role for subplate neurons in the patterning of connections from thalamus to neocortex. Development. 1993;117:1031–1047.
29. Rivkin MJ, Flax J, Mozell R, Osathanondh R, Volpe JJ, Villa-Komaroff L, Oligodendroglial development in human fetal cerebrum. Ann Neurol. 1995 Jul; 38(1):92-101.

30. Hardy RJ, Friedrich VL Jr, Oligodendrocyte progenitors are generated throughout the embryonic mouse brain, but differentiate in restricted foci. Development. 1996 122:2059-2069.
31. Pegueroles J, Vilaplana E, Montal V, Sampedro F, Alcolea D, Carmona-iragui M, et al. Longitudinal brain structural changes in preclinical Alzheimer disease Alzheimers Dement, 13 (2017), pp. 499-509
32. Lee JS, Park YH, Park S, Yoon U, Choe Y, Cheon BK, et al. Distinct brain regions in physiological and pathological brain aging. Frontiers in Aging Neuroscience. 2019;11. https://doi.org/10.3389/fnagi.2019.00147
33. Fortin JP, Parker D, Tunc B, Watanabe T, Elliott MA, Ruparel k, Roalf DR, Satterthwaite TD, Gur RC, Gur RE, Schultz RT, Verma R, Shinohara RT, Harmonization of multi-site diffusion tensor imaging data, Neuroimage, 161 (2017), pp. 149-170
34. Jack CR Jr. et al. NIA-AA research framework: toward a biological definition of Alzheimer's disease. Alzheimers Dement. 14, 535–562 (2018).

Figures

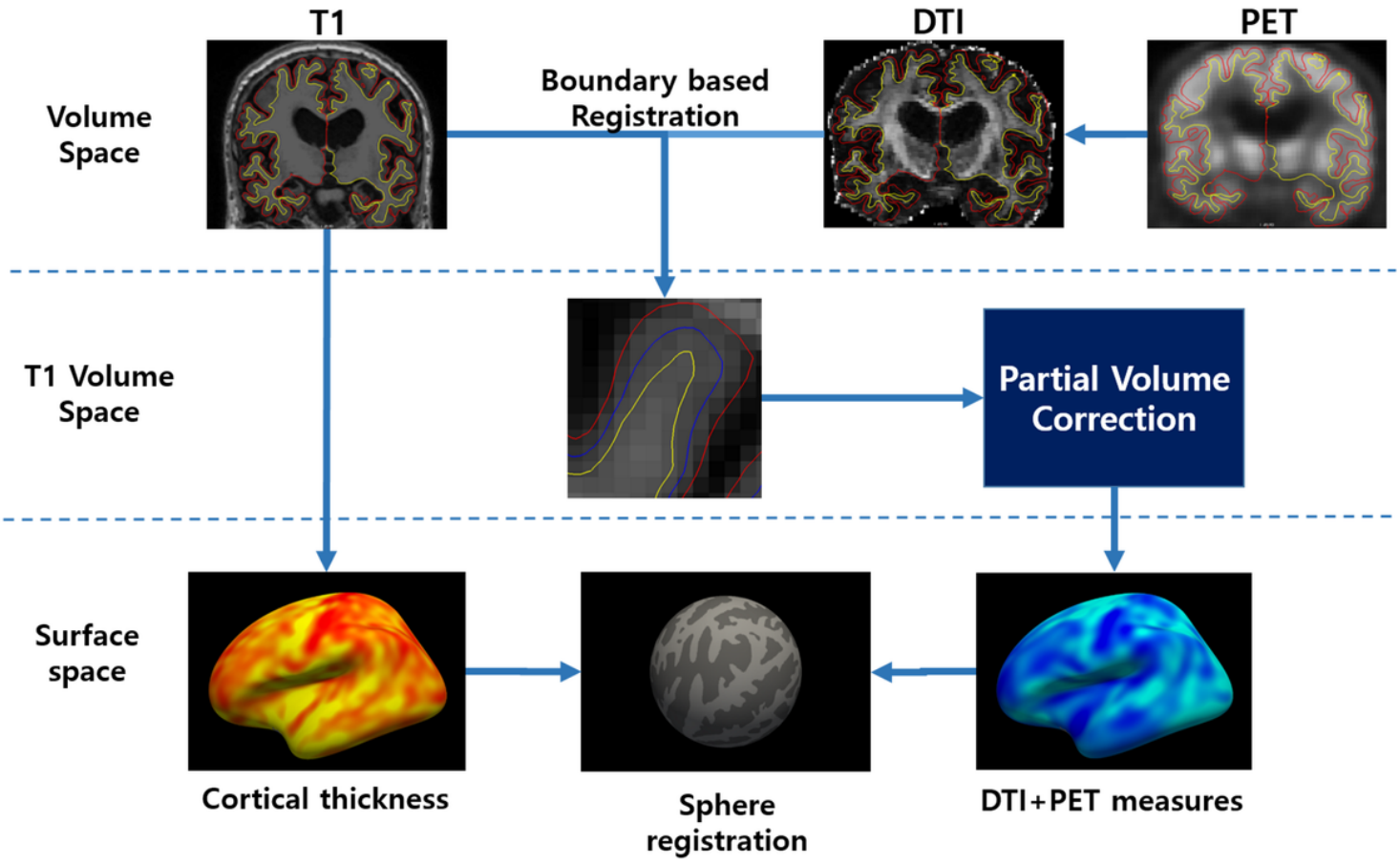

Figure 1

Overall scheme for surface projection analysis. DTI and PET images were boundary-based registered to T1 image and projected to fsaverage surface for group comparison.

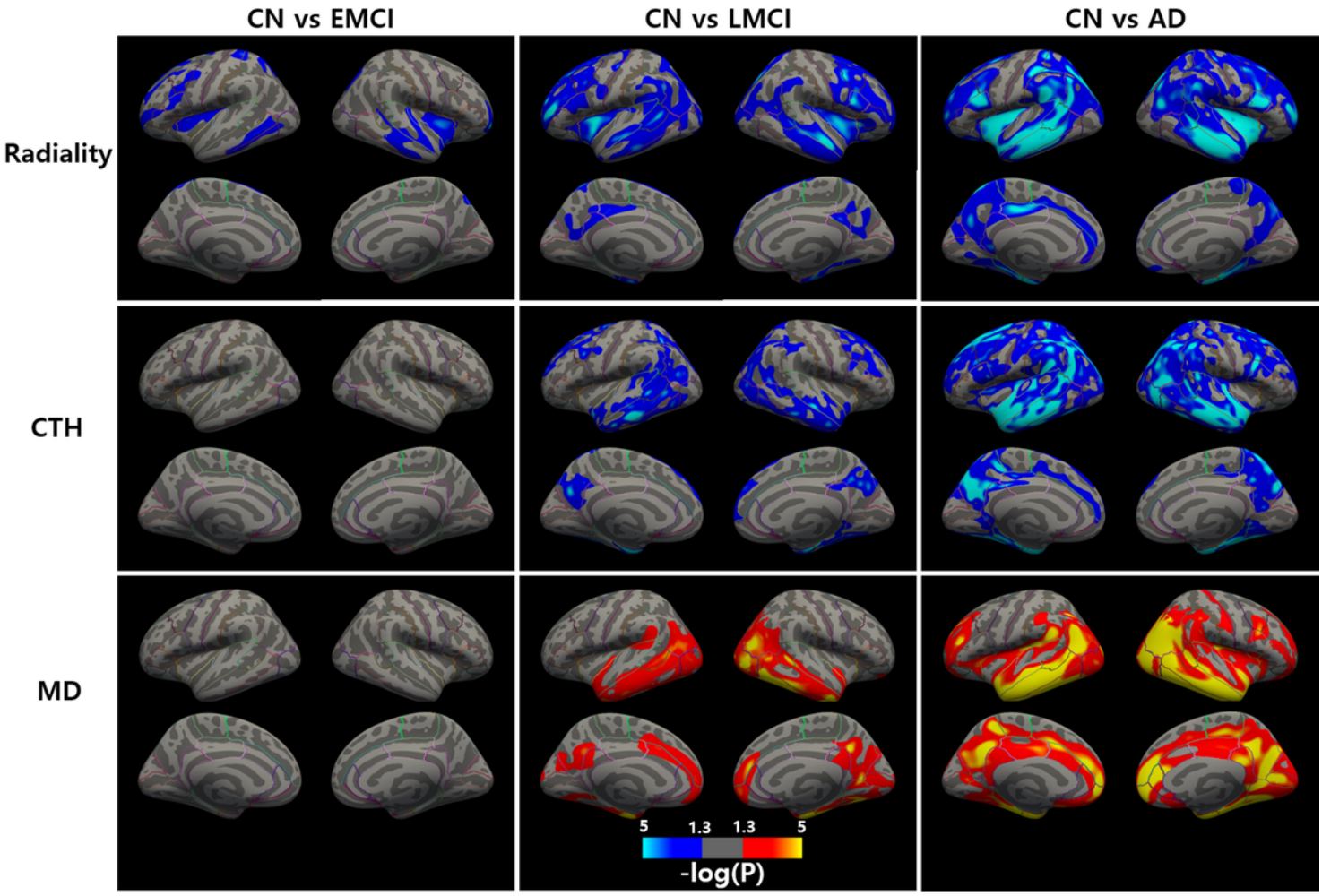

Figure 2

Group differences in radiality, cortical thickness, and mean diffusivity From left to right: CN vs EMCI, CN vs LMCI, and CN vs AD. Blue cluster shows decrease in metrics and red cluster shows increase in metrics. All the cluster were multiple corrected for p-value <0.05. Heat map indicate p-value interval of 0.05 to 10-5

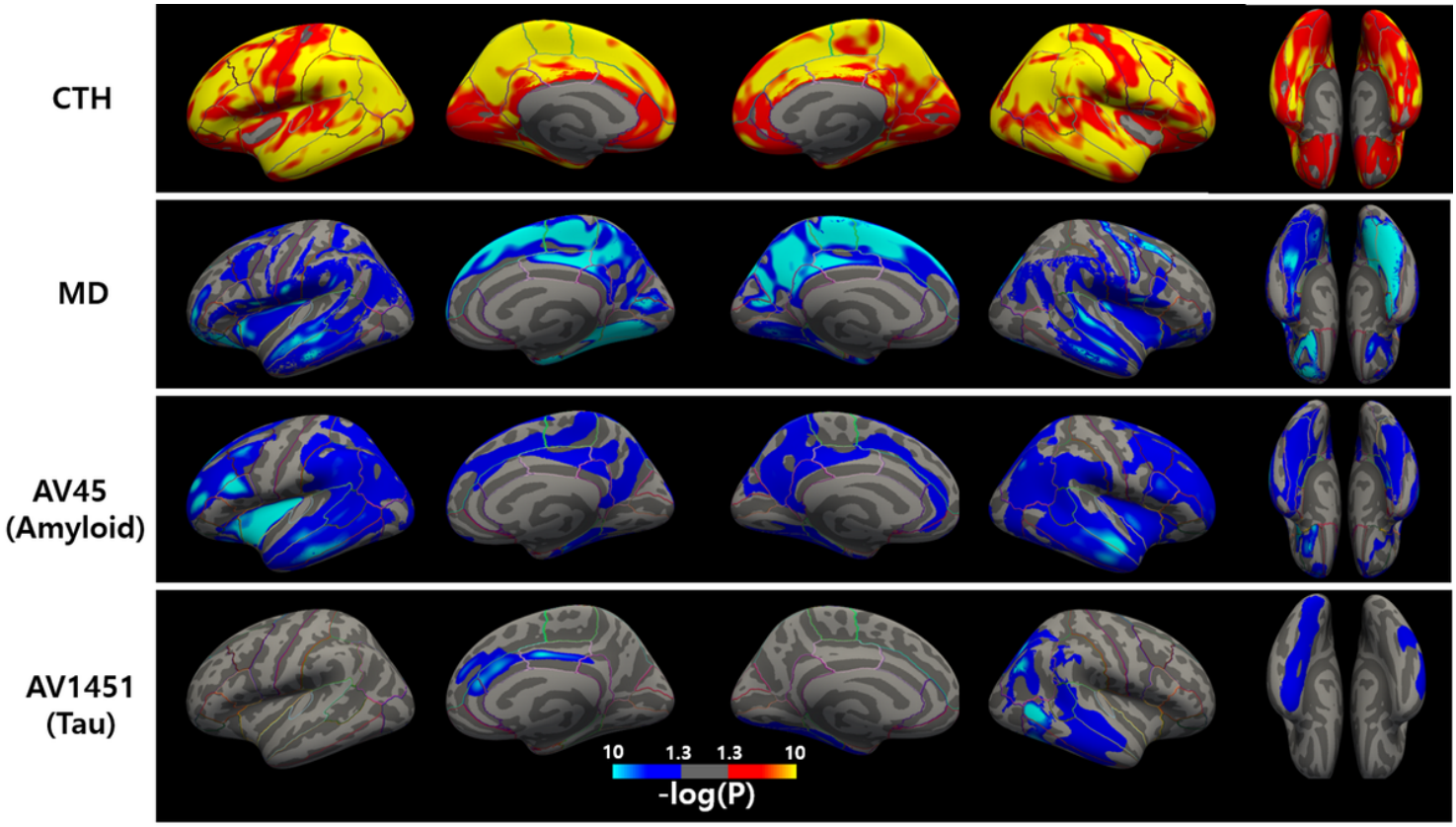

Fig 3. Partial correlation with Radiality

Figure 3

Partial correlation between image biomarkers and radiality. Red cluster shows positive correlation with radiality and blue cluster shows negative correlation. Cortical thickness showed positive correlations, mean diffusivity, AV45, and AV1451 showed negative correlations. Heat map indicate p-value interval of 0.05 to 10-10

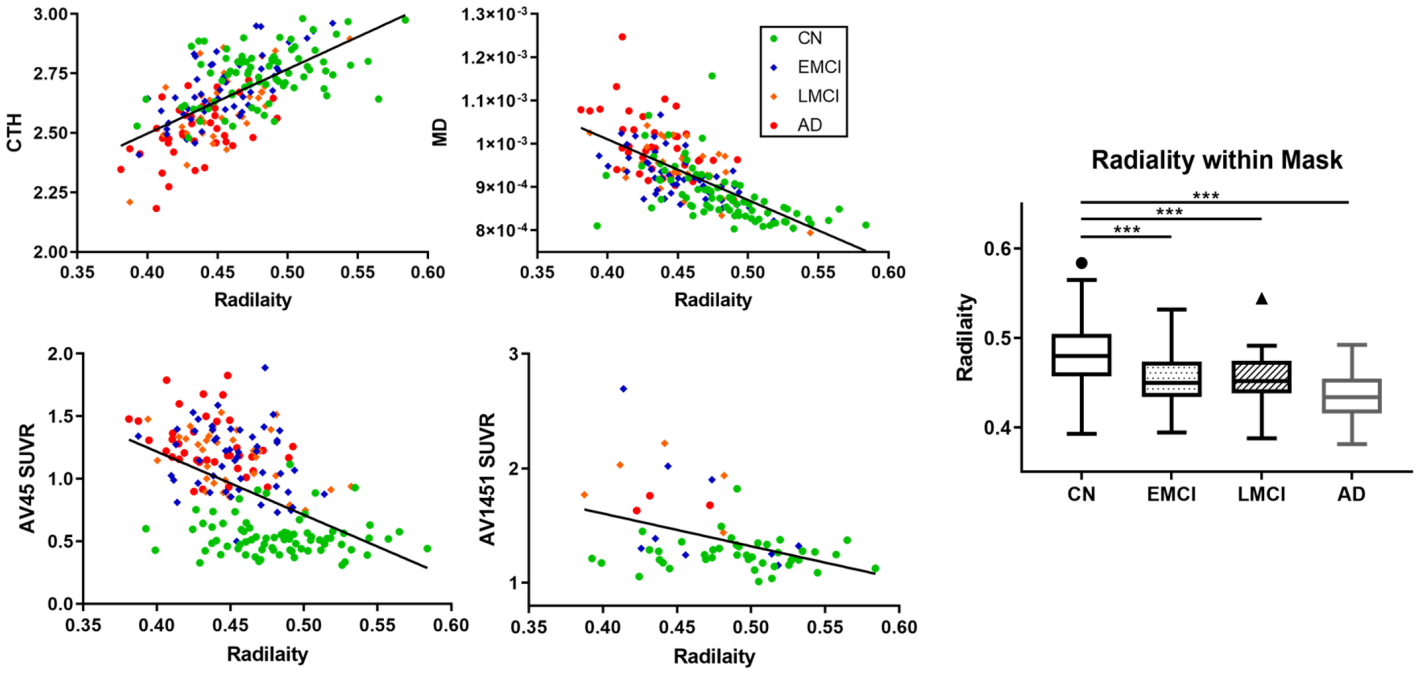

Figure 4

Correlation between radiality with other biomarkers (a) ~ (d) Scatter plot between image biomarkers and radiality. Radiality showed high association with conventional biomarker, indicating that it reflects neuropathology of AD (a) CTh, (b) MD, (c) AV45, (d) AV1451 respectively. (e) Box plot of group radiality comparison within AD specific ROI. Radiality from CN showed significant differences with EMCI, LMCI , and AD with P<0.001. There were no difference in comparing EMCI and LMCI.

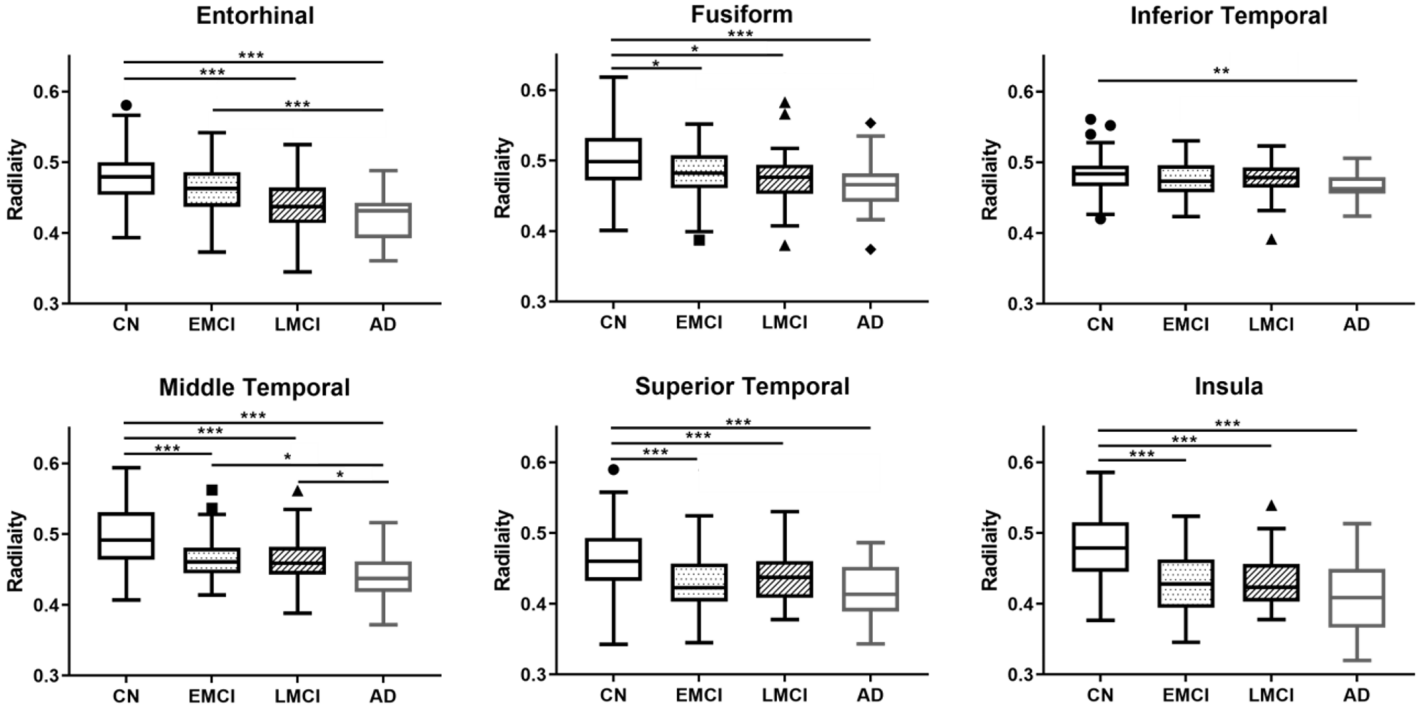

Figure 5

Box plot of group radiality comparison within AD specific ROI. (a) Entorhinal, (b) fusiform, (c) inferior temporal, (d) middle temporal, (e) superior temporal, (f) insula cortex. Significance was tested with two-sample t-test with * P <0.05, ** P <0.01, *** P <0.001

Supplementary Files

This is a list of supplementary files associated with this preprint. Click to download.

- Supplementarymaterials.docx